

# Climate impacts of energy technologies depend on emissions timing

Morgan R. Edwards<sup>1</sup> and Jessika E. Trancik<sup>1,2\*</sup>

**Energy technologies emit greenhouse gases with differing radiative efficiencies and atmospheric lifetimes<sup>1–3</sup>. Standard practice for evaluating technologies, which uses the global warming potential (GWP) to compare the integrated radiative forcing of emitted gases over a fixed time horizon<sup>4</sup>, does not acknowledge the importance of a changing background climate relative to climate change mitigation targets<sup>5,6</sup>. Here we demonstrate that the GWP misvalues the impact of CH<sub>4</sub>-emitting technologies as mid-century approaches, and we propose a new class of metrics to evaluate technologies based on their time of use. The instantaneous climate impact (ICI) compares gases in an expected radiative forcing stabilization year, and the cumulative climate impact (CCI) compares their time-integrated radiative forcing up to a stabilization year. Using these dynamic metrics, we quantify the climate impacts of technologies and show that high-CH<sub>4</sub>-emitting energy sources become less advantageous over time. The impact of natural gas for transportation, with CH<sub>4</sub> leakage, exceeds that of gasoline within 1–2 decades for a commonly cited 3 W m<sup>–2</sup> stabilization target. The impact of algae biodiesel overtakes that of corn ethanol within 2–3 decades, where algae co-products are used to produce biogas and corn co-products are used for animal feed. The proposed metrics capture the changing importance of CH<sub>4</sub> emissions as a climate threshold is approached, thereby addressing a major shortcoming of the GWP for technology evaluation<sup>7,8</sup>.**

Comparing the climate impacts of energy technologies is challenging because they emit differing types and quantities of greenhouse gases, most notably CH<sub>4</sub> and CO<sub>2</sub>, and these gases have dissimilar properties (Fig. 1a,b). Present approaches to technology evaluation use an equivalency metric to convert emissions to their CO<sub>2</sub>-equivalent value<sup>1–3,9</sup>. The most common metric is the global warming potential (GWP( $\tau$ )), which takes the ratio of the time-integrated radiative forcing of pulse non-CO<sub>2</sub> and CO<sub>2</sub> emissions over a fixed time horizon ( $\tau$ ), typically 100 years. The GWP(100) was initially intended as a placeholder<sup>10</sup>, in large part because of its sensitivity to the arbitrarily selected time horizon<sup>7</sup> (Fig. 1c,d), but it remains the standard metric for technology evaluation.

Various alternative metrics have been proposed for the purposes of emissions trading<sup>11–13</sup> and demand-sector emissions evaluations<sup>8,14</sup>. These metrics are formulated to make either instantaneous<sup>15,16</sup> or time-integrated comparisons of gases<sup>1,9</sup>, based on their relative contributions to radiative forcing<sup>1,12</sup>, temperature change<sup>15,16</sup>, or economic impacts<sup>17,18</sup>. Alternatively, some have argued that direct comparisons of gases are not feasible, and have called for a multi-basket emissions policy<sup>5,6</sup>, where similar gases are grouped into baskets and trading between baskets is prohibited.

Technologies emit multiple gases during their life cycles, however, and therefore an equivalency metric is required to compare

their climate impacts on a single scale. For technology evaluation, equivalency metrics must be forward-looking and robust to inherent uncertainties about the future climate scenario, to inform the advanced commitment needed to develop new technologies and infrastructure. Determining an appropriate metric for this application is becoming increasingly urgent as we consider major public and private investments in technologies with significant CH<sub>4</sub> emissions, including natural gas<sup>1,19–22</sup>.

Although many equivalency metrics have been proposed, previous research has not emphasized testing their performance against intended climate goals to determine a principled treatment of time in metric formulations. Here we propose a new class of dynamic metrics that, unlike the static GWP( $\tau$ ), are designed to avoid an overshoot of an intended radiative forcing stabilization level. We develop a method to test the performance of these and other metrics against this climate change mitigation goal. The new metrics differ from other dynamic metrics<sup>16–18</sup> in that they do not require detailed information about the emissions scenario for achieving the mitigation goal. Climate targets are commonly formulated around a stabilization level<sup>23</sup>, which can be reached by a number of emissions scenarios. The proposed metrics are designed to evaluate technologies in this context.

We begin by examining the GWP(100) for later comparison with the new metrics proposed. Although it has been shown that the GWP(100) leads to an imperfect equivalency when used to replace CO<sub>2</sub> with CH<sub>4</sub> (ref. 5), and can lead to economically inefficient decisions in scenarios with exogenously constrained climate outcomes<sup>24</sup>, its performance has not been tested against intended climate goals. We find that using the GWP(100) leads to a significant overshoot of radiative forcing stabilization targets. For example, on the basis of the GWP(100), compressed natural gas (CNG) seems to have an advantage over gasoline per kilometre travelled (Fig. 1c). However, in a hypothetical scenario in which CNG is used to meet US passenger vehicle energy demand, radiative forcing is significantly higher than GWP(100)-based projections suggest (Fig. 2a). In a scenario in which global transportation demand is supplied by an energy source with the CH<sub>4</sub> intensity of CNG, a stabilization target of 3 W m<sup>–2</sup> is exceeded by almost 5% (Fig. 2b), and by 12% if CH<sub>4</sub> emissions are maintained at their present percentage of global CO<sub>2</sub>-equivalent emissions. These errors become increasingly concerning over time as climate thresholds are approached.

The metrics developed here aim to address this concern by appropriately evaluating technologies with significant CH<sub>4</sub> emissions. The objective is to limit the risk of a significant and sustained overshoot of an intended radiative forcing stabilization level.

The first metric, the CCI, is based on the time-integrated radiative forcing from the emission time ( $t'$ ) to an intended

<sup>1</sup>Engineering Systems Division, Massachusetts Institute of Technology, 77 Massachusetts Avenue, Cambridge, Massachusetts 02139, USA, <sup>2</sup>Santa Fe Institute, 1399 Hyde Park Road, Santa Fe, New Mexico 87501, USA. \*e-mail: [trancik@mit.edu](mailto:trancik@mit.edu)

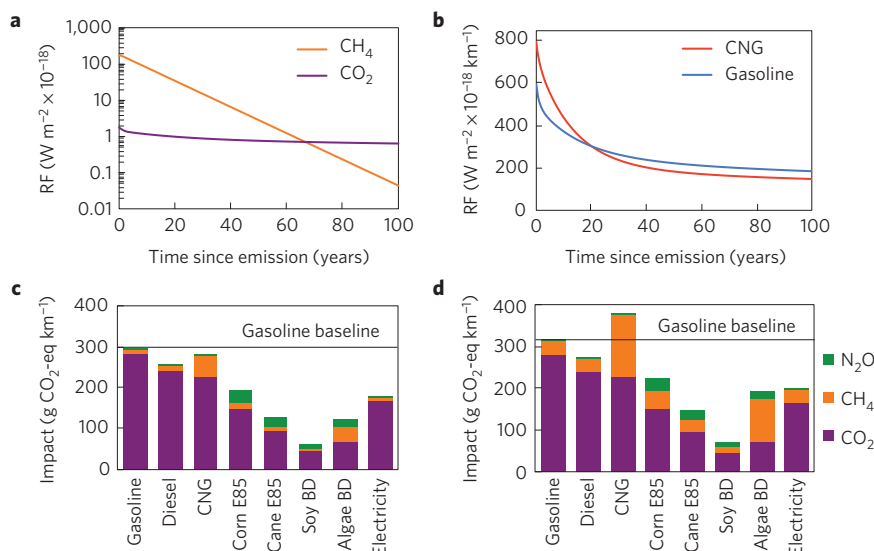


**Figure 1 | Comparisons of greenhouse gases and technologies depend on the evaluation horizon.** **a**,  $\text{CH}_4$  has 102 times the radiative forcing per gram of  $\text{CO}_2$  but decays more quickly, with the gases having equal radiative forcing (RF) 67 years after emission<sup>4</sup>. **b**, As a result, the impact of using technologies decays over time at different rates, as the comparison of gasoline and CNG illustrates. **c,d**, These dynamics explain why the impacts of technologies, notably algae biodiesel with a biogas co-product, change when evaluated over a 100-year (**c**) versus a 20-year (**d**) time horizon. (BD, biodiesel; CNG, compressed natural gas.)

stabilization time ( $t_s$ ) and the second metric, the ICI, on the radiative forcing at time  $t_s$ :

$$\text{CCI}(t', t_s) = \frac{A_M \int_{t'}^{t_s} f_M(t'', t') dt''}{A_K \int_{t'}^{t_s} f_K(t'', t') dt''} \quad \text{for all } t' \leq t_s \quad (1)$$

$$\text{ICI}(t', t_s) = \frac{A_M f_M(t_s, t')}{A_K f_K(t_s, t')} \quad \text{for all } t' \leq t_s \quad (2)$$

where  $A$  is the radiative efficiency,  $f(t, t')$  is the removal function (see equation (5) in Methods), and subscripts  $K$  and  $M$  refer to  $\text{CO}_2$  and  $\text{CH}_4$ , respectively. For emission times  $t' \leq t_s$ , the radiative forcing is evaluated over time  $t''$  (from  $t'$  to  $t_s$ ) for the CCI and at time  $t_s$  for the ICI. For emission times  $t' > t_s$ , both metrics are defined as the instantaneous radiative forcing ratio of the two gases. The CCI places a greater value on  $\text{CH}_4$  emitted before  $t_s$ , after which time the two metrics are equivalent.

These dynamic metrics, in contrast to the static  $\text{GWP}(\tau)$ , explicitly account for climate stabilization goals in their formulation (Supplementary Section 2.1). As the emission time ( $t'$ ) nears the intended stabilization time ( $t_s$ ), the evaluation time horizon decreases and the  $\text{CO}_2$ -equivalent value of  $\text{CH}_4$  increases, to limit the overshoot of the intended stabilization level. (Any overshoot arises from  $\text{CH}_4$  rather than  $\text{CO}_2$  emissions, because  $\text{CO}_2$  emissions are evaluated directly, not through an equivalency metric (Supplementary Section 3).) Unlike previously proposed dynamic metrics (Supplementary Section 2.2), including those comparing the cost effectiveness of emissions reductions along a mitigation scenario<sup>17</sup> and those based on temperature<sup>15,16,18</sup>, the CCI and ICI are formulated so that the only input they require on the climate scenario is the intended radiative forcing stabilization level. A set of possible stabilization years is determined based on this level, giving a range of metric values for each emission year.

The approach developed to compute the metrics and test their performance is illustrated with an example below. The approach involves developing reference scenarios for emissions and radiative forcing stabilization (equations (3)–(6) in Methods and Supplementary Section 1.1), calculating metric values

for the reference scenario range (equations (1) and (2) and Supplementary Section 2.1), and testing metrics against the reference scenarios (equations (7) and (8) in Methods and Supplementary Section 1.2 and 3).

To calculate the emission-time-dependent CCI and ICI values, a range of possible scenarios is determined for a commonly cited  $3 \text{ W m}^{-2}$  radiative forcing threshold (Fig. 3a), which in equilibrium is associated with a  $2^\circ\text{C}$  temperature change. These scenarios define a range of years when radiative forcing must stabilize to avoid exceeding  $3 \text{ W m}^{-2}$ . This roughly 15-year range defines the possible values of  $t_s$  for calculating the CCI and ICI. Figure 3b shows the CCI and ICI for this range of  $t_s$  values.

We simulate emissions decisions using the ICI, CCI and  $\text{GWP}(100)$  to test the metrics' performance. Figure 3c,d shows the results under two scenarios that span the set of feasible scenarios for a  $3 \text{ W m}^{-2}$  stabilization level. Radiative forcing remains below

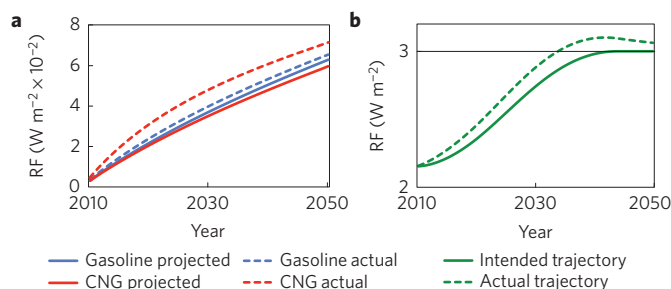


**Figure 2 | GWP(100) underestimates the radiative forcing contribution of  $\text{CH}_4$ -emitting technologies.** **a**, The actual radiative forcing (RF) impacts of satisfying constant US passenger vehicle energy demand with gasoline versus compressed natural gas (CNG) differ from GWP(100)-based projections, with a greater discrepancy for CNG due to its higher  $\text{CH}_4$  intensity. **b**, A hypothetical situation is shown (based on scenario C in Fig. 3a), in which global transportation emissions are replaced by emissions from a technology with the  $\text{CH}_4$  intensity of CNG, using the GWP(100) to determine  $\text{CO}_2$  equivalence (Supplementary Section 1.2). This results in a significant deviation from the intended radiative forcing scenario.

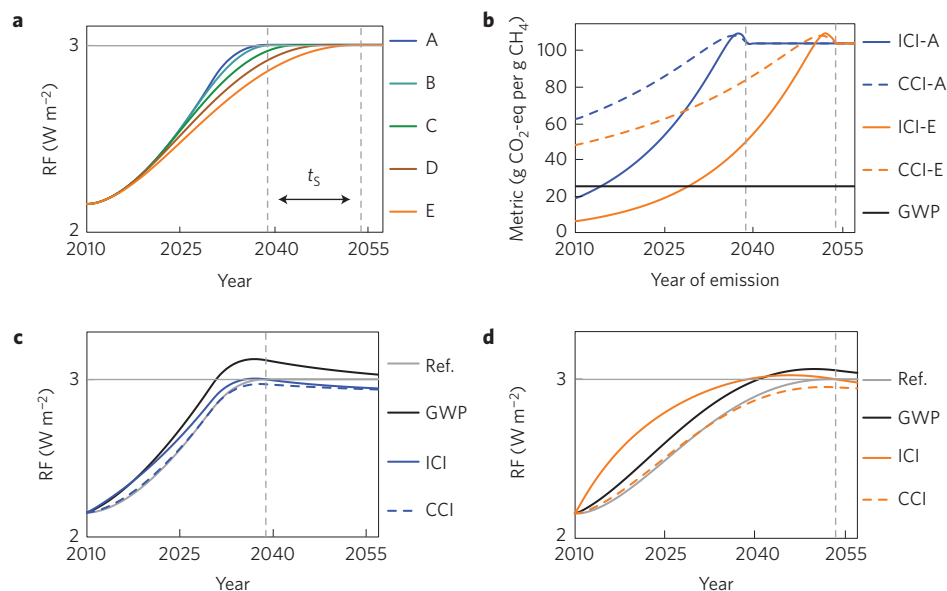


**Figure 3 | Metric development.** **a**, A range of scenarios, consistent with a  $3 \text{ W m}^{-2}$  stabilization level, is used to calculate equivalency metrics. They range from a delay scenario followed by rapid emissions reductions (scenario A,  $t_s = 2039$ ), to a gradual emissions reduction scenario (scenario E,  $t_s = 2054$ ). **b**, We compare the valuation of  $\text{CH}_4$  under the ICI, CCI and GWP(100), using A and E to represent the range of scenarios consistent with the  $3 \text{ W m}^{-2}$  threshold. **c,d**, The radiative forcing (RF) resulting from using these metrics to allocate 5% of  $\text{CO}_2$ -equivalent emissions to  $\text{CH}_4$  is shown, using scenario A (**c**) and scenario E (**d**).

$3 \text{ W m}^{-2}$  for all scenarios using the CCI but exceeds this value using the GWP(100). Using the ICI under scenario E, a gradual emissions reduction scenario with a later  $t_s$ , radiative forcing temporarily exceeds  $3 \text{ W m}^{-2}$  before  $t_s$  because of a lower impact value placed on  $\text{CH}_4$  emissions early on (Supplementary Section 3). Radiative forcing remains below this level when applying the ICI under scenario A, a delay scenario followed by rapid emissions reductions. Both the ICI and CCI avoid the sustained threshold overshoot that results from applying the GWP(100), with the ICI resulting in a temporary overshoot for some scenarios and the CCI preventing any overshoot.

Using the GWP(100) and the CCI/ICI with  $t_s$  defined by scenario C (Fig. 3a), we then compare the climate impacts of several prominent energy technologies (where technology refers to a fuel and conversion technology) that emit both  $\text{CH}_4$  and  $\text{CO}_2$ . Pairwise comparisons are performed for gasoline and CNG, corn ethanol and algae biodiesel (with corn co-products used for animal feed and algae co-products used to produce biogas), and coal and natural gas electricity (Fig. 4 and Supplementary Fig. 9 for other comparisons). We also generate low- $\text{CH}_4$  emissions scenarios for the three high- $\text{CH}_4$  emitters (CNG, algae biodiesel and natural gas electricity) and compare the results with our baseline scenario (Supplementary Sections 4 and 5). Results for the low- $\text{CH}_4$  scenarios are indicated by curly brackets. Notably, for the two pairs of transportation technologies, the rank ordering of climate impact depends on the emissions time.

Initially the impact of CNG is lower than that of gasoline, based on the ICI, but then exceeds it in 6–21 {18–28} years, or 11 {24} years for scenario C. The more conservative CCI, in contrast, indicates a lower CNG impact in all years {after 9–21 years}. Algae biodiesel shows a significantly lower impact than corn ethanol initially, but then surpasses it in 23–38 years when applying the ICI and 21–35 years when applying the CCI, owing to  $\text{CH}_4$  emissions in the production of biogas from algae co-products. The impact of algae biodiesel remains lower than corn ethanol for all years, however, under the low- $\text{CH}_4$  emissions scenario, highlighting the importance of co-product processing techniques in determining the climate impacts of biofuels. Natural gas electricity

starts at 53% {52%} the climate impact of electricity from coal (using the ICI), but then rises to 82% {72%} the impact of coal over time.

We then simulate the radiative forcing resulting from several hypothetical scenarios where all US passenger vehicle energy demand is met with a single technology. These simulations approximate how technologies are assessed through the lens of each metric. Figure 5a compares the results to the sector radiative forcing budget, again determined using scenario C (from Fig. 3a). Figure 5b shows the corresponding vehicle kilometres travelled. Assessing technologies with the GWP(100) results in a large radiative forcing budget overshoot, due to relatively high energy consumption, which endures past  $t_s$  (Supplementary Section 3). Applying the ICI results in a significantly lower and more temporary overshoot that is reduced before  $t_s$ , concurrent with a decrease in energy consumption. Application of the more conservative CCI avoids a threshold overshoot and results in the lowest energy consumption.

These results shed light on technology evaluation debates. One debate focuses on natural gas<sup>19,20</sup>. Using the GWP(100), the US natural gas mix has a slight climate advantage over gasoline, although this conclusion depends on assumptions about the source of the gas and associated emissions, with unconventional natural gas having higher emissions during well construction but conventional gas generally having higher emissions during production<sup>21</sup>. Based on the ICI and CCI, CNG used today ranges from slightly advantageous to slightly disadvantageous, whereas CNG used in 2040 has a significantly higher climate impact and lower climate-goal-compliant consumption than gasoline. These general conclusions also hold under the low- $\text{CH}_4$  emissions scenario (Supplementary Section 5.1).

Another debate focuses on the climate benefits of various biofuels and co-product processing techniques. For the processes studied (Fig. 4b), algae biodiesel seems more favourable than corn ethanol in 2010. However, using the ICI and CCI we observe that by 2040 the climate impact of algae biodiesel surpasses that of corn ethanol, owing to  $\text{CH}_4$  leakage in biogas production from algae co-products, which partially offsets the energy requirements

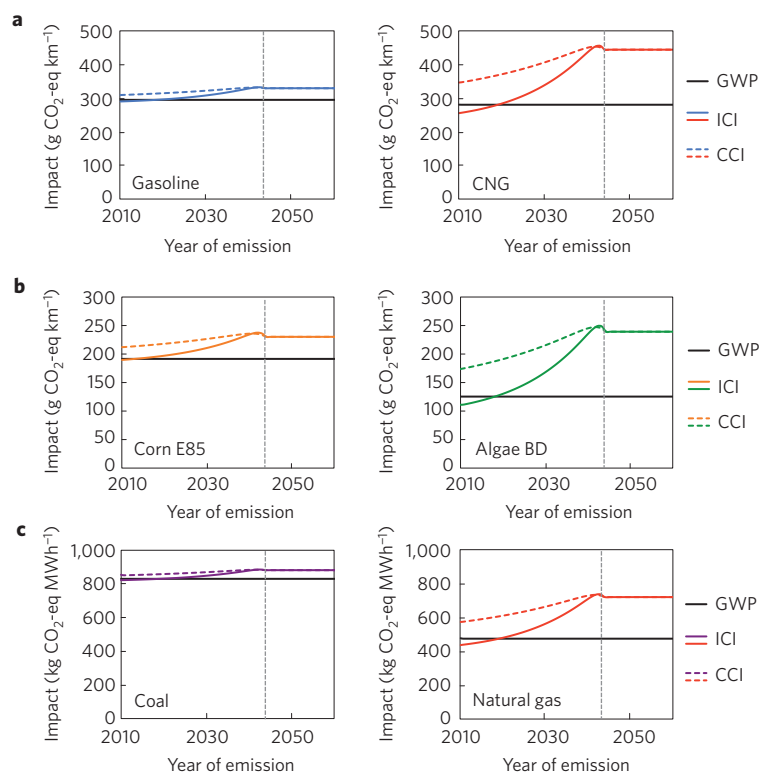


**Figure 4 | Technology comparisons.** **a–c**, Gasoline and compressed natural gas (CNG) with CH<sub>4</sub> leakage (**a**), corn ethanol without and algae biodiesel (BD) with biogas production (**b**), and coal- and natural gas-fired electricity (**c**) are compared using the GWP(100), ICI and CCI. The relative impacts change over time. Under baseline CH<sub>4</sub> emissions assumptions, the impact of CNG overtakes that of gasoline after 11 years when applying the ICI using scenario C in Fig. 3a, and 6–21 years based on the full range of stabilization scenarios investigated. Algae biodiesel overtakes corn ethanol after 28 years for scenario C and the ICI, and 23–38 years based on all scenarios.

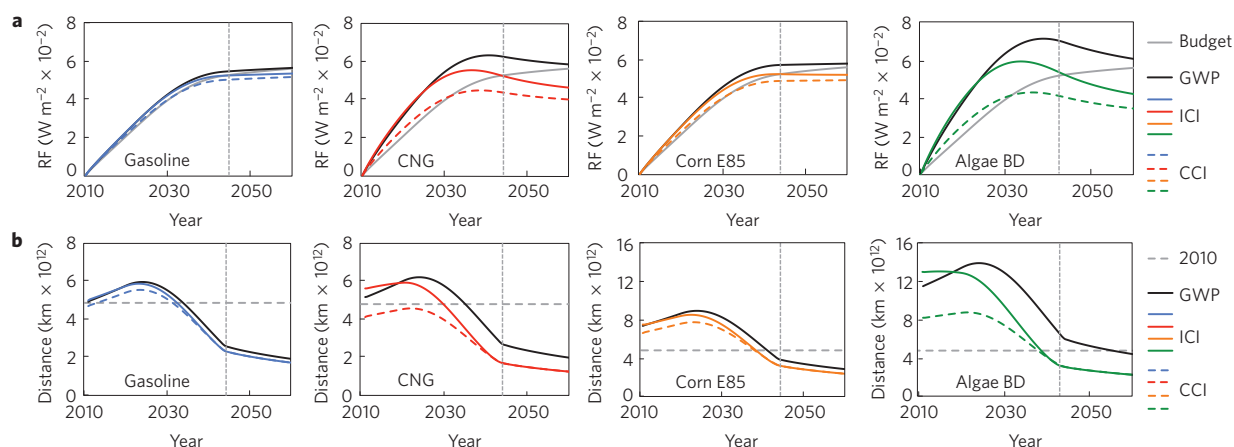


**Figure 5 | Simulations of radiative forcing and vehicle kilometres travelled.** **a, b**, Using metrics to examine hypothetical technology pathways results in differing radiative forcing trajectories, as compared with the sector budget (**a**), and differences in vehicle kilometres travelled (**b**). The sector budget is calculated by allocating a percentage of global emissions, based on scenario C (Fig. 3a), to the US passenger vehicle sector, based on the present value ( $\sim 3\%$ ), and simulating the associated radiative forcing (RF) (Supplementary Section 1.2.2). The metric-based radiative forcing is determined by using a metric to calculate emissions and associated energy consumption levels. Average present vehicle efficiencies and driving patterns are assumed (Supplementary Section 4).

of algae production and processing<sup>2</sup>. Although these offsets make biodigestors attractive, with applications in corn ethanol production<sup>25</sup> and other biofuels, resulting CH<sub>4</sub> emissions may make this process less advantageous over time. An alternative catalytic hydrothermal gasification process may achieve much lower CH<sub>4</sub> emissions (Supplementary Fig. 8). These results suggest the importance of developing alternative low-CH<sub>4</sub> co-product processing techniques<sup>26</sup>.

The CCI and ICI identify high-CH<sub>4</sub>, low-CO<sub>2</sub> technologies as candidates for near-term but not long-term climate change mitigation. Based on an intended radiative forcing stabilization level, these metrics identify an approximate bridging timeline to transition away from CH<sub>4</sub>-emitting, short-term mitigation technologies. The approximate bridging time is not particularly scenario dependent, owing to the constrained range of emissions scenarios and stabilization years that correspond to commonly



cited stabilization targets. The results of applying the metrics to CH<sub>4</sub>-emitting algae biodiesel and natural gas for electricity and transportation are particularly notable, highlighting the dependence of their mitigation potential on their time of use. The proposed technology and metric evaluation approach can also be adapted to new information on the timing, location and form of climate thresholds<sup>23,27,28</sup>, and the desired trade-off between the risks of exceeding thresholds and the benefits of economic activity<sup>29</sup> (Supplementary Section 2.2). Although no equivalency metric is perfect, we find that dynamic metrics that are based on an approximate climate stabilization target and corresponding time horizon can improve technology evaluation for policymaking, private investment and engineering design.

## Methods

In this section we describe the approach to generating the reference scenarios used to calculate the range of CCI and ICI values and to test metric performance. We also describe the technology emissions data used in the research.

**Reference scenarios.** The reference scenarios are CO<sub>2</sub> emissions, multi-gas concentration scenarios: all emissions in the simulation are composed entirely of CO<sub>2</sub>, but previous emissions of non-CO<sub>2</sub> greenhouse gases are also modelled (Supplementary Section 1.1). These reference scenarios are used to calculate the CCI and ICI and to test all metrics, by allocating a portion of CO<sub>2</sub>-equivalent emissions to non-CO<sub>2</sub> gases using the metrics.

Emissions scenarios are constructed<sup>30</sup>, where initial emissions  $e_0$  change over time according to

$$e(t') = e_0 \exp \left[ \int_0^{t'} g(t'') dt'' \right] \quad (3)$$

where  $g(t'')$  is an evolving, exponential growth rate ( $t''$  is a dummy, integration variable). Emissions grow at a constant rate  $g_0$ , based on present growth rates, until the mitigation onset time ( $t_i$ ), after which  $g(t'')$  is reduced by a fixed annual amount until it reaches the final growth rate  $g_f$ .

Concentrations  $c_i(t)$  of each gas  $i$  are a function of pre-industrial concentrations  $c_i(t_0)$ , historical emissions ( $t_0 < t' \leq 0$ ) and new emissions ( $0 < t' \leq t$ ),

$$c_i(t) = c_i(t_0) + \int_0^t f_i(t, t') e_i(t') dt' + \int_0^{t'} f_i(t, t') e_i(t') dt' \quad (4)$$

where  $f_i(t, t')$  gives the fraction of a gas emitted at  $t'$  remaining at time  $t$  (ref. 4),

$$f_i(t, t') = a_0 + \sum_{j=1}^n a_j \cdot \exp \left( -\frac{t-t'}{\tau_j} \right) \quad (5)$$

and  $a_j$  and  $\tau_j$  are constants (see Supplementary Table 2 for CO<sub>2</sub>, CH<sub>4</sub> and N<sub>2</sub>O values). (Equation (5) is also used in the CCI and ICI formulations (equations (1) and (2)), where  $t$  is replaced by  $t''$  for the CCI, which ranges from  $t'$  to  $t_s$ , and is replaced by  $t_s$  for the ICI.) As  $n=1$  and  $a_0=0$  for non-CO<sub>2</sub> greenhouse gases, no information about the emissions timing is needed to calculate concentrations from historical emissions. For CO<sub>2</sub>, where  $n=3$  and  $a_0 \neq 0$ , the rate of removal must be approximated using historical emissions data (Supplementary Section 1.1.2).

Radiative efficiency (radiative forcing per unit concentration) values are used to determine radiative forcing from concentrations<sup>4</sup>.

$$RF(t) = RF_A(t) + \sum_i [A_i [c_i(t) - c_i(0)] + RF_i(c_i(0))] \quad (6)$$

where  $RF_A(t)$  refers to all radiative forcing not due to the presence of modelled gases  $i$ , and  $A_i$  is the radiative efficiency of gas  $i$  (Supplementary Section 1.1.3).

A scenario family is a set of pathways  $RF(t)$  that stabilize at the same radiative forcing threshold but approach it at different rates. To generate stabilization scenarios, emissions are adjusted after the threshold is reached such that radiative forcing equals the threshold value in all subsequent years. Emissions scenarios within a scenario family are defined based on their values of  $t_1$ , which is varied to the greatest extent possible. Earlier values of  $t_1$  result in gradual emissions reductions, whereas later values of  $t_1$  result in delayed emissions reductions followed by rapid reductions. The scenario family for 3 W m<sup>-2</sup> stabilization defines the range of stabilization times ( $t_s$ ) for the analysis presented in the paper.

**Metric testing.** The performance of emissions metrics is tested by budgeting a trajectory  $e(t')$  for total CO<sub>2</sub>-equivalent emissions, and allocating a fraction  $q$  of these emissions to a non-CO<sub>2</sub> greenhouse gas. Consider the case of two gases, CO<sub>2</sub> and CH<sub>4</sub>. Given a metric  $\mu(t')$ , the sum of CO<sub>2</sub> emissions  $e_K(t')$  and CO<sub>2</sub>-equivalent CH<sub>4</sub> emissions  $\mu(t')e_M(t')$  must equal  $e(t')$ . The radiative forcing scenario can be derived from equation (6),

$$\begin{aligned} RF(t) = & A_K \left[ \left( c_K(t_0) + c_{KL}(t) + (1-q) \int_0^t e(t') f_K(t, t') dt' \right) - c_K(0) \right] + RF_K(c_K(0)) \\ & + A_M \left[ \left( c_M(t_0) + c_{ML}(t) + q \int_0^t e(t') f_M(t, t') \cdot \frac{1}{\mu(t')} dt' \right) - c_M(0) \right] \\ & + RF_M(c_M(0)) + RF_A(t) \end{aligned} \quad (7)$$

where K and M subscripts refer to CO<sub>2</sub> and CH<sub>4</sub> respectively, all other contributions to radiative forcing are encompassed in the term  $RF_A(t)$ , and concentrations are disaggregated into the three contributions given in equation (4): pre-industrial concentrations, concentrations from historical emissions (abbreviated  $c_{iL}(t)$ ), and concentrations from new emissions. The difference between the actual radiative forcing in the mixed gas case (where  $q \neq 0$ ) and the budgeted, CO<sub>2</sub> emissions case (where  $q=0$ ) is

$$\Delta RF(t) = q \int_0^t e(t') \left[ A_M f_M(t, t') \cdot \frac{1}{\mu(t')} - A_K f_K(t, t') \right] dt' \quad (8)$$

A similar approach is used to test metric performance for technology evaluation, given a budgeted emissions trajectory  $e(t')$  and using historical data to allocate a fraction  $p$  of these emissions to the sector of interest (Supplementary Section 1.2.2).

**Data.** Global emissions, concentration and radiative forcing data are published by the International Institute for Applied Systems Analysis. Technology life-cycle emissions are taken from the Greenhouse Gases, Regulated Emissions, and Energy Use in Transportation (GREET) Version 2012, published by Argonne National Laboratory. In GREET, natural gas CH<sub>4</sub> emissions that arise from liquid unloading in conventional production offset increased leakage during unconventional well completion, with conventional gas having 27% higher emissions than unconventional gas. Present US breakdowns of conventional and unconventional gas are used<sup>22</sup>. In GREET, corn co-products are used as animal feed and algae co-products are used to create biogas in a state-of-the-art facility with CH<sub>4</sub> leakage rates of 2% (ref. 2). Emissions for electricity generation technologies are taken from a recent study<sup>1</sup>. Low-CH<sub>4</sub> emissions scenarios for natural gas are based on updated EPA estimates of natural gas system leakage and an alternative catalytic hydrothermal gasification scenario for algae biodiesel<sup>2</sup> (Supplementary Section 4).

Received 27 September 2013; accepted 20 March 2014;  
published online 25 April 2014; corrected after print  
25 April 2014

## References

- Alvarez, R. A., Pacala, S. W., Winebrake, J. J., Chameides, W. L. & Hamburg, S. P. Greater focus needed on methane leakage from natural gas infrastructure. *Proc. Natl Acad. Sci. USA* **109**, 6435–6440 (2012).
- Frank, E. D., Han, J., Palou-Rivera, I., Elgowainy, A. & Wang, M. Q. Methane and nitrous oxide emissions affect the life-cycle analysis of algal biofuels. *Environ. Res. Lett.* **7**, 1–10 (2012).
- Stratton, R. W., Wolfe, P. J. & Hileman, J. I. Impact of aviation non-CO<sub>2</sub> combustion effects on the environmental feasibility of alternative jet fuels. *Environ. Sci. Technol.* **45**, 10736–10743 (2011).
- Solomon, S. et al. (eds) *Climate Change 2007: The Physical Science Basis* (Cambridge Univ. Press, 2007).
- Daniel, J. S. et al. Limitations of single-basket trading: Lessons from the Montreal Protocol for climate policy. *Climatic Change* **111**, 241–248 (2011).
- Smith, S. M. et al. Equivalence of greenhouse-gas emissions for peak temperature limits. *Nature Clim. Change* **2**, 8–11 (2012).
- Azar, C. & Johansson, D. J. A. Valuing the non-CO<sub>2</sub> climate impacts of aviation. *Climatic Change* **111**, 559–579 (2011).
- Peters, G. P., Aamaas, B., Lund, M. T., Solli, C. & Fuglestad, J. S. Alternative 'global warming' metrics in life cycle assessment: A case study with existing transportation data. *Environ. Sci. Technol.* **45**, 8633–8641 (2011).

9. Kendall, A. Time-adjusted global warming potentials for LCA and carbon footprints. *Int. J. Life Cycle Ass.* **17**, 1042–1049 (2012).
10. Shine, K. P. The global warming potential—the need for an interdisciplinary retrieval. *Climatic Change* **96**, 467–472 (2009).
11. Tanaka, K., Johansson, D. J. A., O'Neill, B. C. & Fuglestedt, J. S. Emissions metrics under a 2 °C stabilization target. *Climatic Change* **117**, 933–941 (2013).
12. Fuglestedt, J. S. *et al.* Metrics of climate change: Assessing radiative forcing and emission indices. *Climatic Change* **58**, 267–331 (2003).
13. Tol, R. S. J., Berntsen, T. K., O'Neill, B. C., Fuglestedt, J. S. & Shine, K. P. A unifying framework for metrics for aggregating the climate effect of different emissions. *Environ. Res. Lett.* **7**, 044006 (2012).
14. Fuglestedt, J. S. *et al.* Transport impacts on atmosphere and climate: Metrics. *Atmos. Environ.* **44**, 4648–4677 (2010).
15. Shine, K. P., Fuglestedt, J. S., Hailemariam, K. & Stuber, N. Alternatives to the global warming potential for comparing climate impacts of emissions of greenhouse gases. *Climatic Change* **68**, 281–302 (2005).
16. Shine, K. P., Berntsen, T. K., Fuglestedt, J. S., Skeie, R. B. & Stuber, N. Comparing the climate effect of emissions of short- and long-lived climate agents. *Phil. Trans. R. Soc. A* **365**, 1903–1914 (2007).
17. Manne, A. S. & Richels, R. G. An alternative approach to establishing trade-offs among greenhouse gases. *Nature* **410**, 675–677 (2001).
18. Johansson, D. J. A. Economics- and physical-based metrics for comparing greenhouse gases. *Climatic Change* **110**, 123–141 (2012).
19. Howarth, R. W., Santoro, R. & Ingraffea, A. Methane and the greenhouse-gas footprint of natural gas from shale formations. *Climatic Change* **106**, 679–690 (2011).
20. Allen, D. T. *et al.* Measurements of methane emissions at natural gas production sites in the United States. *Proc. Natl Acad. Sci. USA* **110** (2013).
21. Weber, C. L. & Calvin, C. Life cycle carbon footprint of shale gas: Review of evidence and implications. *Environ. Sci. Technol.* **46**, 5688–5695 (2012).
22. Burnham, A. *et al.* Life-cycle greenhouse gas emissions of shale gas, natural gas, coal, and petroleum. *Environ. Sci. Technol.* **46**, 619–627 (2011).
23. United Nations Framework Convention on Climate Change. Report of the Conference of the Parties on its fifteenth session, held in Copenhagen from 7 to 19 December 2009, FCCC/CP/2009/11/Add.1.
24. Ekholm, T., Lindroos, T. J. & Savolainen, I. Robustness of climate metrics under climate policy ambiguity. *Environ. Sci. Policy* **31**, 44–52 (2013).
25. Liska, A. J. *et al.* Improvements in life cycle energy efficiency and greenhouse gas emissions of corn-ethanol. *J. Ind. Ecol.* **13**, 58–74 (2009).
26. Scott, S. A. *et al.* Biodiesel from algae: Challenges and prospects. *Curr. Opin. Biotechnol.* **21**, 277–286 (2010).
27. Alley, R. B. *et al.* Abrupt climate change. *Science* **299**, 2005–2010 (2003).
28. Lenton, T. M. Beyond 2 °C: Redefining dangerous climate change for physical systems. *WIREs Clim. Change* **2**, 451–461 (2011).
29. Lenton, T. M. *et al.* Tipping elements in the Earth's climate system. *Proc. Natl Acad. Sci. USA* **105**, 1786–1793 (2008).
30. Allen, M. R. *et al.* Warming caused by cumulative carbon emissions towards the trillionth tonne. *Nature* **458**, 1163–1166 (2009).

## Acknowledgements

The authors thank J. McNerney for his contributions to the development of the metric testing model. We thank S. Solomon for helpful feedback on this manuscript. This research was partially financially supported by the New England University Transportation Center at MIT under DOT grant No. DTRT07-G-0001.

## Author contributions

J.E.T. developed the concept and designed the methods for the study, M.R.E. and J.E.T. performed the analysis, J.E.T. and M.R.E. wrote the paper.

## Additional information

Supplementary information is available in the [online version of the paper](#). Reprints and permissions information is available online at [www.nature.com/reprints](http://www.nature.com/reprints). Correspondence and requests for materials should be addressed to J.E.T.

## Competing financial interests

The authors declare no competing financial interests.